Yuan 2.0-M32: A MoE model with Localized Filtering-based Attention and Attention Router

Anonymous ACL submission

Abstract

In this work, we develop and release Yuan 2.0-M32, a language model uses a mixture-of-experts architecture with 32 experts of which 2 experts are active. The Localized Filtering-Based Attention (LFA) is introduced to the base architecture, to incorporate prior knowledge of local dependencies of natural language into attention. A new router network, Attention Router, is adopted for a more efficient selection of experts, which improves the accuracy compared to the model with classical router network. A distributed training method with nonuniform pipeline parallel, data parallel, and optimizer parallel is proposed, which greatly reduces the bandwidth requirements of intranode communication, and achieves good performance in large-scale distributed training. Yuan 2.0-M32 is trained with 2000B tokens from scratch, and the training computation consumption is only 9.25% of a dense model at the same parameter scale.

1 Introduction

Given a fixed amount of computation for each token, a model with Mixture of Experts (MoE) structure can be easily built on a much larger scale than a dense model by increasing the number of experts, and thus achieves a higher accuracy performance. In reality, it is common to train a model with limited computational resource, and the MoE is considered as a good candidate to reduce the substantial cost associated with the extreme large scale of model, datasets and limited computing power. In recent years, with the ever-increasing model size, the role of routing strategy has attracted more attention for efficient allocation of computation resources.

The experts routing network is the core in a MoE structure. This structure selects candidate experts to participate in the computation by calculating the probability of token allocation to each expert. Currently, in most popular MoE structures, it is common to adopt a classical routing algorithm that performs a dot product between the token and the feature vector representing each expert, and then selects the experts with the largest dot product value (Shazeer et al., 2017; Fedus et al., 2022; Zhou et al., 2022). The feature vectors of the experts in this transformation are independent, ignoring the correlation between experts. However, the MoE structure usually select more than one expert each time, and multiple experts often participate in calculation collaboratively, which means there should be an inherent correlation between experts. It will undoubtedly improve the accuracy of the model, if the relationship between experts is considered in the process of selecting experts.

Attention, as a basic block in LLMs, has shown great successes across NLP tasks (Vaswani et al., 2017; Raffel et al., 2020). The vanilla attention mechanism treats all tokens equally regardless of the distance. However, in natural language, the dependencies of words in the neighborhood are often stronger than those far away. The interconnection learned by vanilla Attention is global without any prior knowledge of local dependencies. EMA, widely used in modeling time-series data, captures local dependencies that decay exponentially over time. MEGA introduced inductive bias into the attention mechanism with the classical EMA method (Ma et al., 2022). In MEGA, the EMA computes over the entire range of input sequence length (or chunk size lengths if chunking is applied) to achieve a strong inductive bias between tokens. Unlike the EMA in MEGA, Yuan 2.0-M32 introduces hierarchical 1-dimensional convolutions into Attention, which brings higher accuracy and computing performance than MEGA.

The major contribution of our work are summarized as follows:

- Propose the Attention Router that considers the correlation between experts, resulting in a

higher accuracy compared with the classical router structure.

- Introduce the Localized Filtering-based Attention into the base architecture of model.

- Design a parallel paradigm with non-uniform pipeline parallelism, data parallelism, and optimizer parallelism. The new parallel paradigm significantly reduces the requirements for communication bandwidth compared to the classical 3D parallel paradigm.

- Release the Yuan 2.0-M32 model with 40B total parameters and 3.7B active ones. There are 32 experts in total and 2 experts activated for each token. The computational consumption for training is only 1/16 of that for a dense model at a similar parameter scale, and the cost for inference is similar to a dense model with 3.7B parameters.

2 Related Work

Gshard (Lepikhin et al., 2021), a giant model with over 600 billion parameters, introduces the MoE method into Transformer Encoder for the first time, and provides an efficient distributed parallel computing architecture with routing across accelerators. Switch Transformer (Fedus et al., 2022) simplifies the MoE routing algorithm with sparse routing. Zhou et al. (2022) has proposed a new MoE routing algorithm called Expert Choice (EC) routing algorithm to achieve the optimal load balancing in the MoE system. Mistral 8x7B model surpasses model with 10 times larger parameters in several human benchmarks with classical routing network (Jiang et al., 2024). DBRX uses a fine-grained MoE architecture and chooses 4 experts among 16 (Mosaic Research Team, 2024). DeepSeekMoE improves the expert specialization with fine-grained expert segmentation as well as shared expert isolation (Dai et al., 2024). The shared experts activate tokens for all inputs and are not affected by the routing module, which may help other experts focus more on their unique domains of knowledge.The above-mentioned works make effort on optimizing the routing strategy of experts, while the router network is still the classical one that ignores the correlation between experts.

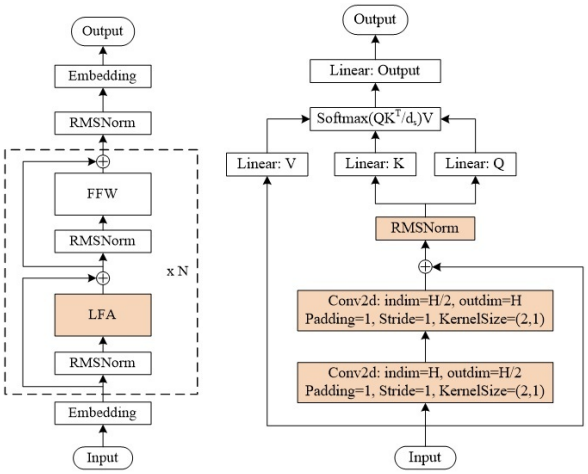

Figure 1: Base model of Yuan 2.0-M32 and the Localized Filtering-based Attention (LFA)

3 Model Architecture

3.1 Localized Filtering-based Attention (LFA)

In the self-attention mechanism of Transformer, contextual information is captured from the entire sequence by modeling interactions pairwise among input tokens. Instead of assuming a prior knowledge of the inter-dependencies between tokens (e.g. positional inductive bias), the self-attention mechanism learns to predict attention weights pairwise from the data, short of neighboring local associations of tokens. In natural language, local dependencies of input tokens are often stronger than those far from each other. This work presents the Localized Filtering-based Attention to favor local dependencies. The LFA introduces inductive bias into the self-attention pairwise weights computation with two consecutive 1-dimensional convolutions (Figure 1). The convolutions in the LFA have one-sided one-dimensional kernel to prevent information in the future tokens from leaking into the current one. The details of convolutions in the LFA are shown in Figure 2. In each LFA block, a token establishes a relationship with two previous tokens. We place an RMSNorm module as the pre-norm before the output embedding that shares the same parameters with the input embedding. SwiGLU (Touvron et al., 2023) plays as the non-linear feed-forward layer in the base model.

We perform an ablation study on the LFA architecture. Table 1 lists the accuracy of models with different architectures of Attention on an internal code dataset. The basic attention has the same architecture with LLaMA. We first add an EMA layer before the calculation of the query and key arrays

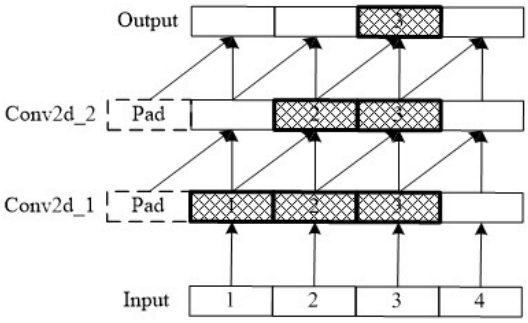

Figure 2: Illustration of convolutions in LFA.

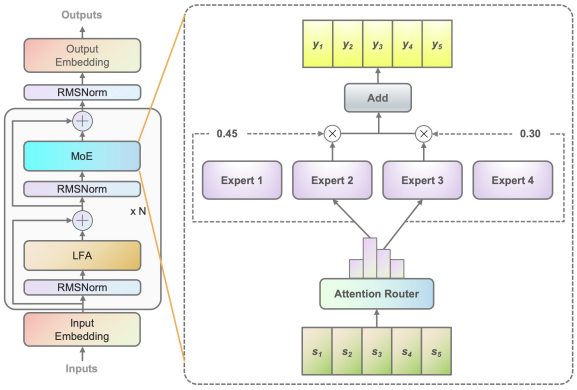

Figure 3: Illustration of Yuan 2.0-M32. Figure on the left showcases the scaling of Yuan 2.0 architecture with MoE layers. The MoE layer takes the place of the feed forward layer in Yuan 2.0. Figure on the right showcases the MoE layer structure. In our model, each input token will be assigned to 2 experts of the total 32, while in the figure we display 4 experts as an example. The output of the MoE is the weighted summation of the selected experts. N is the number of layers.

in self-Attention. The test loss improves by 1.6%, while the running time increases by 29%. Such large overhead is unacceptable in a large model training. In the LFA, one-sided 1-dimensional convolution kernels with different kernel sizes are tested. The best accuracy is obtained with a kernel size of 7. The test loss is improved by 3.3% compared to the basic model, with the parameters increased by 15%. In order to lower the memory consumption during LLM training, we reduce the kernel size of the two convolution kernels to 2, and the accuracy is close to the kernel size of 7. Then, we add the RMSNorm after two convolutions, and the accuracy is further improved. The LFA with two convolutions and an RMSNorm is applied in the base model of Yuan 2.0-M32, and the test loss improvement is 3.5% compared to the baseline.

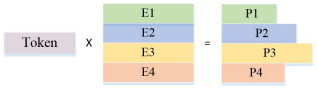

(a) Classical router

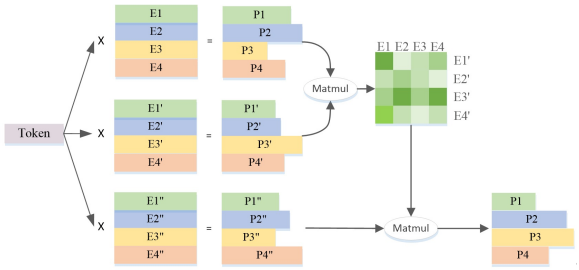

(b) Attention router

Figure 4: The overview of the attention router structure.

3.2 Attention router

When the base model is adopted in a sparse architecture, the dense feed-forward network (FFN) of every layer is replaced with a MoE component.

Figure 3 displays the architecture of MoE layer applied in our model. Taking four FFNs as an example (32 experts in fact), each MoE layer is composed of a group of individual FFNs as experts. The Router network ahead of experts dispatches the input token to the relevant expert(s). The classic Router network essentially establishes a feature vector for each expert, and computes the dot product between input token and the feature vector of each expert to obtain the specific likelihoods between token and experts. The experts with the strongest likelihood are selected for activation and participate in subsequent calculations.

Figure 4a presents the structure of classical router network. The feature vectors of each expert are independent from each other, and the correlation between experts is ignored when calculating the probability. In fact, in most MoE models (Lepikhin et al., 2021; Fedus et al., 2022; Zhou et al., 2022), two or more experts are usually selected to participate in the subsequent calculations, which naturally brings a strong correlation between experts. The consideration of correlation between experts will undoubtedly contribute to the improvement of accuracy.

Figure 4b presents the architecture of the Attention Router, a novel router network proposed in this work, incorporate correlation between experts by taking Attention mechanism. A coefficient matrix representing the correlation between experts is built, and then applied on the computation for the

Model		Params/M	Time per iter/ms	Test Loss
Attention (basic)		160.3	577	1.251
Attention with EMA		160.6	745	1.2309
LFA	Conv kernel size[1,1,h,h]	163.9	596	1.2444
	Conv kernel size[2,1,h,h]	167.4	602	1.2194
	Conv kernel size[3,1,h,h]	171.0	605	1.2171
	Conv kernel size[7,1,h,h]	185.1	621	1.2093
	Two Conv kernels, size[2,1,h,h/2],[2,1,h/2,h]	167.4	618	1.2122
	+RMSNorm	167.4	631	1.2069

Table 1: Test losses on different attention architecture. All the models have the same number of layers and hidden dimensions. Attention with EMA refers to an EMA layer (Ma et al., 2022) inserted into Attention in a similar way as the convolutions in the LFA.

final probability value. In specific, given N experts for a token vector ($I \in \mathbb{R}^d$), the expert routing process is as follows:

$$\begin{cases} Q = WI, & W \in \mathbb{R}^{N \times d} \\ K = W^{'}I, & W^{'} \in \mathbb{R}^{N \times d} \\ V = W^{''}I, & W^{''} \in \mathbb{R}^{N \times d} \\ P = Softmax(QK^T)V, & P \in R^N \end{cases} \quad (1)$$

Then, the M experts are chosen by selecting top M values of P. In this paper, we set $M = 2$, $N = 32$, $d = 2048$.

Our model is tested on 8 trainable experts with the Attention Router. The classical router model has 8 trainable experts to ensure a similar parameter scale, and the router structure is the same with that applied in Mixtral 8x7B (Jiang et al., 2024), which is a Softmax over a linear layer. The Shared Expert router takes the strategy of Shared Expert Isolation with classical router architecture (Dai et al., 2024). There are 2 fixed experts to capture the common knowledge and top-2 of 14 optional experts as the specialized ones. The output of MoE is the combination of the fixed and the ones selected by router. All the three models are trained with 30B tokens and tested with another 10B tokens. Considering the results between classical router and Shared Expert router, we find that the latter one gets exactly the same test loss with 7.35% more training time. The computational efficiency of the Shared Expert is relatively low, and it does not bring better training accuracy over the classical MOE strategy. Thus in our model, we take the classical routing strategy without any shared experts.

We test the scalability of the model by increasing number of experts and fixing the per-expert parameter size. The increase in the number of trainable experts only changes the model capacity, but not the actual activated model parameters. All the models are trained with 50B tokens and tested with another 10B tokens. We set the activated experts as 2, and the hyper-parameters for training are the same for the three models. The expert scaling effects is measured by the test loss after trained with 50B tokens (Table 2). Compared to the model with 8 trainable experts, model with 16 experts displays 2% lower loss, and model with 32 experts displays 3.6% lower loss. We choose 32 experts for Yuan 2.0-M32 considering its accuracy.

Model	Test loss
8 experts	1.820
16 experts	1.787
32 experts	1.754

Table 2: Results of the scaling experiments.

4 Training

4.1 Pre-training

Distributed training of large models often involves tensor parallelism, pipeline parallelism, and data parallelism (named Method 1). Tensor parallel requires multiple global collective communications (e.g. AllReduce) during each forward and backward propagation. Communication greatly increases the bandwidth requirements between AI chips and would be a performance bottleneck for LLM training. For models with similar architecture with GPT-3 or LLaMA, we build a model to calculate the time consumption of a single iteration with the 3D parallel method (tensor parallelism, pipeline parallelism and data parallelism) with the following equation:

$$
\begin{aligned}
T_{M1} = & \underbrace{\frac{96ABLSH^2\left(1+\frac{S}{6H}\right)}{P_s * T_s * F}}_{T_0} \\
& + \underbrace{\frac{96ABLSH^2\left(1+\frac{S}{6H}\right)}{P_s * T_s * F} * \frac{(P_s-1)}{A}}_{T_1} \\
& + \underbrace{\frac{8ABSH}{n_{net} * BW_{net}}}_{T_2} + \underbrace{48 * \frac{L*(T_s-1)}{P_s * T_s * BW_{\text{link}}} ABSH}_{T_3} \\
& + \underbrace{12LH^2\left(1+\frac{13}{12H}+\frac{V}{12LH}\right) * \frac{8*(D_s-1)/D_s}{P_s * n_{net} * BW_{net}}}_{T_4}
\end{aligned}
\tag{2}
$$

while for Yuan 2.0-M32 with LFA, the time consumption of a single iteration can be obtained with the following equation:

$$
\begin{aligned}
T_{M1} = & \underbrace{\frac{144ABLSH^2\left(1+\frac{S}{8H}\right)}{P_s * T_s * F}}_{T_0} \\
& + \underbrace{\frac{144ABLSH^2\left(1+\frac{S}{8H}\right)}{P_s * T_s * F} * \frac{(P_s-1)}{A}}_{T_1} \\
& + \underbrace{\frac{8ABSH}{n_{net} * BW_{net}}}_{T_2} + \underbrace{48 * \frac{L*(T_s-1)}{P_s * T_s * BW_{\text{link}}} ABSH}_{T_3} \\
& + \underbrace{16LH^2\left(1+\frac{1}{8}+\frac{7}{32H}+\frac{V}{16LH}\right) * \frac{8*(D_s-1)/D_s}{P_s * n_{net} * BW_{net}}}_{T_4}
\end{aligned}
\tag{3}
$$

The differences between Eq. (2) and Eq. (3) come mainly from the LFA. The details of each part in Eq. (2) are listed in Table A. The Yuan 1.0-245B with the similar architecture as GPT-3 is trained on a GPU cluster (2128 GPUs) with computing efficiency of 45%. The time predicted by Eq.(2) is 44.33s per time step of Yuan 1.0 training, and the average measured time is 46.20s. If we want to achieve the same performance for dense Yuan with LFA at a similar scale, the bidirectional bandwidth of the tensor parallelism would be 730 GB/s, which is much greater than the theoretical bandwidth of pipeline or data parallelism, which is 43 GB/s.

In order to reduce the communication bandwidth and achieve high performance on low-bandwidth intra- and interconnection, we propose a distributed training method that trains LLMs with pipeline parallelism, data parallelism, and optimizer parallelism (named Method 2).

In pipeline parallelism, uniform partitioning is often applied, which refers to even divisions of the Transformer layers onto each computing device. In order to hide communication, it is often necessary to allocate a larger memory at the beginning of the pipeline to store temporary variables, and the required memory will exceed the GPU memory limit.Taking a 24-layer transformer model with

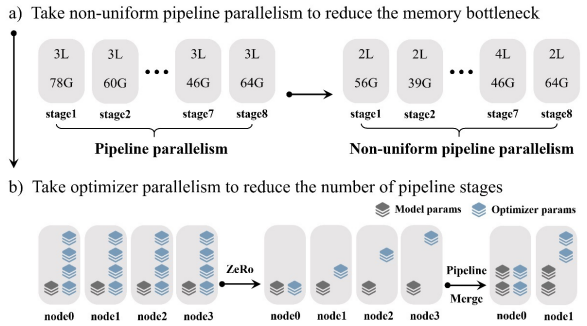

Figure 5: Illustration of non-uniform parallelism and optimizer parallelism.

hidden_size=6144 as an example, the model is divided into 8 pipeline stages. If we follow the traditional pipeline parallelism, the 24 layers will be uniformly divided, and each pipeline stage is assigned with 3 layers. When using checkpoint activation, the first pipeline stage will cache 24 activations for backpropagation, while in the last pipeline stage, only 3 activations will be cached for backpropagation. The maximum memory consumption is about 78GB (Figure5), which is quite close to GPU memory limit. If we further increase the number of layers, we have to increase the number of pipeline stages, which requires more computation devices and leads to lower performance. In order to address this issue, this work proposes a **non-uniform pipelining parallel** method, which splits the layers non-uniformly to break the memory bottleneck. In this way, we can split the 24 layer transformer into 8 pipeline stages of [2, 2, 3, 3, 4, 4, 4, 2] layers, and the memory usage of the first pipeline stage drops to 56GB. About 28.2% memory saves compared to the original pipeline parallelism. In order to further reduce the memory consumption, we propose a **block-wise cross-entropy computation** method that reduces the peak memory consumption of cross-entropy calculations with a large vocab size in the last pipeline stage. With this method, the $logits \in R^{S\times H}$ are split into $logits_{block} \in R^{block_{size}\times H}$, and the loss of each block is calculated individually, then concatenated together. This approach enables us to meet the memory needs of the last pipeline stage without additional computing or communication. The time consumption for the blockwise cross-entropy computation method is calculated with Eq. (4),

$$
\begin{aligned}
T_{M2} = & \underbrace{\frac{96AB\boldsymbol{L}SH^2\left(1+\frac{S}{6H}\right)}{\boldsymbol{P}_s * \boldsymbol{F}}}_{T_0} \\
& + \underbrace{\frac{96AB\boldsymbol{L}SH^2\left(1+\frac{S}{6H}\right)}{\boldsymbol{P}_s * F}\frac{(P_s-1)}{A}}_{T_1} + \underbrace{\frac{8ABSH}{BW_{link}}}_{T_2} \\
& + \underbrace{12LH^2\left(1+\frac{13}{12H}+\frac{V}{12LH}\right) * \frac{8*(D_s-1)/D_s}{P_s * n_{net} * BW_{net}}}_{T_4}
\end{aligned} \tag{4}
$$

And for Yuan with LFA, the time consumption is calculated as,

$$
\begin{aligned}
T_{M2} = & \underbrace{\frac{144AB\boldsymbol{L}SH^2\left(1+\frac{S}{8H}\right)}{\boldsymbol{P}_s * \boldsymbol{F}}}_{T_0} \\
& + \underbrace{\frac{144AB\boldsymbol{L}SH^2\left(1+\frac{S}{8H}\right)}{\boldsymbol{P}_s * F}\frac{(P_s-1)}{A}}_{T_1} + \underbrace{\frac{8ABSH}{BW_{link}}}_{T_2} \\
& + \underbrace{16LH^2\left(1+\frac{1}{8}+\frac{7}{32H}+\frac{V}{16LH}\right) * \frac{8\,(D_s-1)/D_s}{P_s * n_{net} * BW_{net}}}_{T_4}
\end{aligned} \tag{5}
$$

Yuan 2.0-M32 is trained with Method 2. We benchmark the performance on a GPU cluster. The prediction made by Eq(5) is quite close to the real measurement with an error of 1.5%, and the the final training loss is 1.22.

Table 3 presents the performance predicted with Eq(5) for the model on a cluster of 96 and 256 AI chips. Considering almost all the P2P bandwidths, the performance of Method 2 is better than that of Method 1. The performance drops up to 37.20% for Method 1 when the P2P BW drops from 400 GB/s to 100 GB/s, while the performance almost keeps the same, only drops 0.23%, for Method 2.

4.2 Fine-tuning

During fine-tuning, we extend the sequence length to 16,384. Following the work of CodeLLama (Rozière et al., 2023), we reset the base value of Rotary Position Embedding (RoPE) frequencies to avoid the decay in attention scores with longer sequences. Instead of simply increasing the base value from 1000 to a much larger value (e.g. 1,000,000), we calculate the new base with the NTK-aware (bloc97, 2023), i.e.

$$
b^{'} = b \cdot s^{\frac{|D|}{|D|-2}} \tag{6}
$$

Where b is the original base value ($b = 10000$). s is the number of extended times from the original context length to the extended context length. As we extend the context length from 4,096 to 16,384, s equals 4. $|D|$ is 128 in our setup. Therefore, the new base $b^{'}$ is calculated to be 40,890.

We also compare the performance of the pre-trained Yuan 2.0-M32 model with the NTK-aware styled new base, and with other base values from 40,000 to 10,240,000) in the needle-retrieval task with sequence lengths up to 16K (Gkamradt, 2023). We find that the NTK-aware styled new base, 40,890, performed better. Thus 40,890 is applied during fine-tuning.

4.3 Dataset

Yuan 2.0-M32 is pre-trained with a bilingual dataset of 2000B tokens from scratch, then fine-tuned with labeled data across different domains. The original data for pre-training contains more than 3400B tokens, and the weight for each category is adjusted according to the data quality and quantity.

The comprehensive pre-training corpus is composed of:

- 44 constituent sub datasets covering web crawled data, wiki, academic thesis, books, codes, math and formula, and domain-specific expertise. Some of them are open source datasets and the others created by Yuan model.
- Most of the pre-training data in our previous works are also reutilized.

Detailed information about the construction and source of pre-training dataset is available in AppendixC.

The fine-tuning dataset is expanded based on our previous dataset and please refer to the details in AppendixD.

5 Results

We evaluate Yuan 2.0-M32 on Humaneval (Chen et al., 2021) for code generation, GSM8K (Cobbe et al., 2021) and the MATH (Hendrycks et al., 2021b) for mathematical problem solving, ARC (Clark et al., 2018) for scientific knowledge and inference, and MMLU (Hendrycks et al., 2021a) as an integrated benchmark.

5.1 Code generation

The capability of code generation is evaluated with the HumanEval Benchmark. The English prompted is constructed as Appendix E.

The model is expected to complete the function after <sep>. And the generated function will be evaluated with unit tests. The results from zero-shot of Yuan 2.0-M32 and the comparison with

P2P BW GB/s	96 Chips		256 Chips	
	Method 1/s	Method 2/s	Method 1/s	Method 2/s
100	369.85	246.18	145.82	103.77
200	303.00	246.08	120.75	103.63
400	269.57	246.00	108.21	103.53

Table 3: Predicted time consumption with different P2P bandwidth between AI chips. The inter-connection between nodes is 200 Gb/s.

Model	Params (B)	Active Params (B)	HumanEval (zero-shot)
Llama 3-70B	70	70	81.7
Llama 3-8B	8	8	62.2
Phi-3-medium	14	14	62.2
Phi-3-small	7	7	61
Phi-3-mini	3.8	3.8	58.5
Qwen1.5-72B	72	72	68.9
DeepseekV2	236	21	81.1
Mixtral-8×22B	141	39	45.1
Mixtral-8×7B	47	12.9	40.2
Yuan 2.0-M32	40	3.7	74.4
Yuan 2.0-M32	40	3.7	78.1 (14 shots)

Table 4: Comparison of Yuan 2.0-M32 and other models on Hu-manEval pass@1.

Model	Params (B)	Active Params (B)	GSM8K	MATH
Llama 3-70B	70	70	93.0	50.4
Llama 3-8B	8	8	79.6	30
Phi-3-medium	14	14	91.0	-
Phi-3-small	7	7	89.6	-
Phi-3-mini	3.8	3.8	82.5	-
Qwen1.5-72B	72	72	81.9	40.6
DeepseekV2	236	21	92.2	53.9
Mixtral-8×22B	141	39	78.6	41.8
Mixtral-8×7B	47	12.9	58.4	28.4
Yuan 2.0-M32	40	3.7	92.7	55.9

Table 5: Comparison of Yuan 2.0-M32 and other models on GSM8K and MATH.

other models are dis-played in Table 4. The result of Yuan 2.0-M32 are second only to DeepseekV2 (DeepSeek-AI et al., 2024) and Llama3-70B (Meta AI, 2024), and far exceed the other models, even when its active parameters and computational consumptions are much lower than those from others. Compared with DeepseekV2, our model uses less than a quarter of the active parameters and less than a fifth of the computational effort per token, while reaching more than 90% of its accuracy level. And compared with llama3-70B, the gap between model parameters and computation is even greater, and we still reach 91% of its level. Yuan 2.0-M32 demonstrated reliable programming capability with three quarters of the questions passed. Yuan 2.0-M32 are good at few shot leaning. The accuracy of Humaneval is improved to 78.0 by taking 14 shots.

5.2 Math

The math capability of Yuan 2.0-M32 is evaluated with GSM8K and MATH benchmark. A GSM-8K problem has a final numerical solution, and it is run it with 8 shots (Table 5).

MATH is a dataset with 12,500 challenging Mathematical Competition QA problems. Yuan 2.0-M32 produces the final answer with chain of thought (CoT) method with 4 shots. The answers will be extracted from analysis and transformed into a unified format. For numerical results, mathematically equivalent output in all formats are accepted. The answer of `\frac{1}{2}`, 1/2, 0.5, 0.50 are all converted into 0.5 and accepted as the same result. For mathematical expressions, we remove the tab and space symbol, and unified the regular expression of arithmetic operation. For instance, $y = ((2x+1))/5, y = (2x+1)/5, y = 2x/5+1/5$, $y = 0.4x + 0.2$, etc. are all accepted as the same answers. The processed final results are compared with the ground truth answer, and evaluated with EM (exact match) scores.

From the results shown in Table 5, we can see that Yuan 2.0-M32 scores the highest on MATH benchmark. Compared to Mixtral-8×7B, which has 3.48 times larger active parameters than Yuan 2.0-M32, the score of Yuan is even nearly twice as high. On GSM8K, Yuan 2.0-M32 also achieves a score very close to that of Llama 3-70B, and outperforms other models.

5.3 MMLU

The input data for Yuan 2.0-M32 is organized as Appendix E. The text before <sep> is sent to the model, and all answer related to the correct answer or the option label is adopted as true. The results on MMLU demonstrate the capabilities of

Model	Params (B)	Active Params (B)	MMLU
Llama 3-70B	70	70	80.3
Llama 3-8B	8	8	68.4
Phi-3-medium	14	14	78.0
Phi-3-small	7	7	75.7
Phi-3-mini	3.8	3.8	68.8
Qwen1.5-72B	72	72	76.2
DeepseekV2	236	21	77.8
Mixtral-8×22B	141	39	77.8
Mixtral-8×7B	47	12.9	70.6
Yuan 2.0-M32	40	3.7	72.2

Table 6: Comparison of Yuan 2.0-M32 and other models on MMLU.

Model	Params (B)	Active Params (B)	ARC-C
Llama 3-70B	70	70	93.3
Llama 3-8B	8	8	78.6
Phi-3-medium	14	14	91.6
Phi-3-small	7	7	90.7
Phi-3-mini	3.8	3.8	84.9
Qwen1.5-72B	72	72	91.7
DeepseekV2	236	21	92.3
Mixtral-8×22B	141	39	91.3
Mixtral-8×7B	47	12.9	85.9
Yuan 2.0-M32	40	3.7	95.8

Table 7: Comparison of Yuan 2.0-M32 and other models on ARC-Challenge.

our model in different domains. The final accuracy is measured with MC1 (Table 6). Yuan 2.0-M32 outperforms Mixtral-8×7B, Phi-3-mini, and Llama 3-8B in terms of performance.

5.4 ARC

We test our model on the Challenge parts of ARC. The question and options are concatenated directly and separated with <n>, which is prompted as in Appendix E (similar to the pattern of MMLU). The text before <sep> is sent to model, and the model is expected to generate a label or corresponding answer. The generated answer is compared with the ground truth, and the results are calculated with MC1 target.

The results ARC-C are displayed in Table 7, and it shows that Yuan 2.0-M32 excels in solving complex scientific problems—it surpasses Llama3-70B in this benchmark.

From 5.1 to 5.4, we compare our performance to three MoE model (Mixtral family, Deepseek) and six dense models (Qwen (Bai et al., 2023), Llama family and Phi-3 family (Abdin et al., 2024)), to evaluate Yuan 2.0-M32's performance on different domains. Table 7 presents the comparison of Yuan 2.0-M32 with other models on accuracy vs computation. Yuan 2.0-M32 uses only 3.7B active parameters and 22.2 GFlops per token for fine-tuning, which is the most economical, to obtain comparable results or even surpass other models listed in the tables. Table 8 implies the outstanding computational efficiency and performance during inference of our model. The average accuracy of Yuan 2.0-M32 is 79.15 that is competitive with Llama3-70B. And the value of average accuracy / Glops per token is 10.69, which is 18.9 times larger than Llama3-70B.

6 Conclusion

In this work, we introduce Yuan 2.0-M32, a bilingual MoE language model. The architecture of Yuan 2.0-M32 is designed by incorporating Attention with localized filtering and converting classical router to Attention Router, which brings a better accuracy with less computation resources. The proposed distributed training method with nonuniform pipeline parallel, data parallel, and optimizer parallel greatly reduces the bandwidth requirements of intra-node communication, and leads to good performance in large-scale distributed training. Yuan 2.0-M32 uses only 3.7B active parameters and 7.4 GFlops of inference per token, both of which are about 1/19 of Llama3-70B. In ARC-C benchmark, our model excels Llama 3-70B by 2.5 pts with only 5% active parameters. For the MATH benchmark, Yuan 2.0-M32 also achieves the highest score (55.9), surpassing Llama 3-70B by 10% with 5% computation cost. The results imply that our model has outstanding computational efficiency and performance during inference. We release our Yuan 2.0-M32 models at Github for public accessibility, as what we did before, and hope the open source model can benefit the development of LLMs and AI industry ecology.

Limitations

Despite Yuan 2.0-M32's outstanding performance in multiple benchmark tests and significant progress in computational efficiency and performance, we acknowledge that the model still has several limitations. First, while Yuan 2.0-M32 excels

Model	Params (B)	Active Params (B)	GFlops per token (Inference)	GFlops per token (Fine-tune)	Average Accuracy	Average Accuracy /GFlops per token (Inference)
Llama 3-70B	70	70	140	420	79.25	0.57
Llama 3-8B	8	8	16	48	64.15	4.00
Qwen1.5-72B	72	72	144	432	72.6	0.50
DeepseekV2	236	21	42	126	79.05‘	1.88
Mixtral-8×22B	141	39	78	234	72.38	0.93
Mixtral-8×7B	47	12.9	25.8	77.4	60.83	2.36
Yuan 2.0-M32	40	3.7	7.4	22.2	79.15	10.69

Table 8: Comparison of Yuan 2.0-M32 and other models on quality vs size. The mean accuracy is averaged on the scores of GSM-8K, Math, Humaneval, MMLU, and ARC-C.

on benchmarks like MATH and ARC-Challenge, we recognize that its performance may still lag behind some models specifically optimized for these fields in tasks that require complex common-sense reasoning or cross-domain knowledge integration. Second, the training of our model relies heavily on a large-scale bilingual dataset, which may limit its performance in low-resource languages or domains. This is an area where we plan to focus more attention in future work. Finally, although the model demonstrates high computational efficiency, we understand that further optimization of inference speed and memory usage is still needed to meet the demands of real-time interaction and large-scale deployment. Future work will focus on addressing these limitations to further enhance the model's performance and applicability. We are committed to continuous improvement and innovation to overcome these challenges.

References

Marah I Abdin, Sam Ade Jacobs, Ammar Ahmad Awan, Jyoti Aneja, Ahmed Awadallah, Hany Awadalla, Nguyen Bach, Amit Bahree, Arash Bakhtiari, Harkirat S. Behl, Alon Benhaim, Misha Bilenko, Johan Bjorck, Sébastien Bubeck, Martin Cai, Caio César Teodoro Mendes, Weizhu Chen, Vishrav Chaudhary, Parul Chopra, Allie Del Giorno, Gustavo de Rosa, Matthew Dixon, Ronen Eldan, Dan Iter, Amit Garg, Abhishek Goswami, Suriya Gunasekar, Emman Haider, Junheng Hao, Russell J. Hewett, Jamie Huynh, Mojan Javaheripi, Xin Jin, Piero Kauffmann, Nikos Karampatziakis, Dongwoo Kim, Mahoud Khademi, Lev Kurilenko, James R. Lee, Yin Tat Lee, Yuanzhi Li, Chen Liang, Weishung Liu, Eric Lin, Zeqi Lin, Piyush Madan, Arindam Mitra, Hardik Modi, Anh Nguyen, Brandon Norick, Barun Patra, Daniel Perez-Becker, Thomas Portet, Reid Pryzant, Heyang Qin, Marko Radmilac, Corby Rosset, Sambudha Roy, Olatunji Ruwase, Olli Saarikivi, Amin Saied, Adil Salim, Michael Santacroce, Shital Shah, Ning Shang, Hiteshi Sharma, Xia Song, Masahiro Tanaka, Xin Wang, Rachel Ward, Guanhua Wang, Philipp Witte, Michael Wyatt, Can Xu, Jiahang Xu, Sonali Yadav, Fan Yang, Ziyi Yang, Donghan Yu, Chengruidong Zhang, Cyril Zhang, Jianwen Zhang, Li Lyna Zhang, Yi Zhang, Yue Zhang, Yunan Zhang, and Xiren Zhou. 2024. Phi-3 technical report: A highly capable language model locally on your phone. *CoRR*, abs/2404.14219.

Zhangir Azerbayev, Edward Ayers, and Bartosz Piotrowski. 2022. proof-pile. https://github.com/zhangir-azerbayev/proof-pile.

b-mc2. 2023. SQL-Create-Context Dataset. https://huggingface.co/datasets/b-mc2/sql-create-context.

Jinze Bai, Shuai Bai, Yunfei Chu, Zeyu Cui, Kai Dang, Xiaodong Deng, Yang Fan, Wenbin Ge, Yu Han, Fei Huang, Binyuan Hui, Luo Ji, Mei Li, Junyang Lin, Runji Lin, Dayiheng Liu, Gao Liu, Chengqiang Lu, Keming Lu, Jianxin Ma, Rui Men, Xingzhang Ren, Xuancheng Ren, Chuanqi Tan, Sinan Tan, Jianhong Tu, Peng Wang, Shijie Wang, Wei Wang, Shengguang Wu, Benfeng Xu, Jin Xu, An Yang, Hao Yang, Jian Yang, Shusheng Yang, Yang Yao, Bowen Yu, Hongyi Yuan, Zheng Yuan, Jianwei Zhang, Xingxuan Zhang, Yichang Zhang, Zhenru Zhang, Chang Zhou, Jingren Zhou, Xiaohuan Zhou, and Tianhang Zhu. 2023. Qwen technical report. *CoRR*, abs/2309.16609.

bloc97. 2023. NTK-Aware Scaled RoPE allows LLaMA models to have extended (8k+) context size without any fine-tuning and minimal perplexity degradation. https://www.reddit.com/r/LocalLLaMA/comments/14lz7j5/ntkaware.

Byroneverson. 2024. shell-cmd-instruct. https://huggingface.co/datasets/byroneverson/shell-cmd-instruct.

Mark Chen, Jerry Tworek, Heewoo Jun, Qiming Yuan, Henrique Pondé de Oliveira Pinto, Jared Kaplan, Harri Edwards, Yuri Burda, Nicholas Joseph, Greg Brockman, Alex Ray, Raul Puri, Gretchen

Krueger, Michael Petrov, Heidy Khlaaf, Girish Sastry, Pamela Mishkin, Brooke Chan, Scott Gray, Nick Ryder, Mikhail Pavlov, Alethea Power, Lukasz Kaiser, Mohammad Bavarian, Clemens Winter, Philippe Tillet, Felipe Petroski Such, Dave Cummings, Matthias Plappert, Fotios Chantzis, Elizabeth Barnes, Ariel Herbert-Voss, William Hebgen Guss, Alex Nichol, Alex Paino, Nikolas Tezak, Jie Tang, Igor Babuschkin, Suchir Balaji, Shantanu Jain, William Saunders, Christopher Hesse, Andrew N. Carr, Jan Leike, Joshua Achiam, Vedant Misra, Evan Morikawa, Alec Radford, Matthew Knight, Miles Brundage, Mira Murati, Katie Mayer, Peter Welinder, Bob McGrew, Dario Amodei, Sam McCandlish, Ilya Sutskever, and Wojciech Zaremba. 2021. Evaluating large language models trained on code. *CoRR*, abs/2107.03374.

Wenhu Chen, Xueguang Ma, Xinyi Wang, and William W. Cohen. 2023. Program of thoughts prompting: Disentangling computation from reasoning for numerical reasoning tasks. *Trans. Mach. Learn. Res.*, 2023.

Peter Clark, Isaac Cowhey, Oren Etzioni, Tushar Khot, Ashish Sabharwal, Carissa Schoenick, and Oyvind Tafjord. 2018. Think you have solved question answering? try arc, the AI2 reasoning challenge. *CoRR*, abs/1803.05457.

Clinton. 2023. Text-to-sql-v1. https://huggingface.co/datasets/Clinton/Text-to-sql-v1.

Karl Cobbe, Vineet Kosaraju, Mohammad Bavarian, Mark Chen, Heewoo Jun, Lukasz Kaiser, Matthias Plappert, Jerry Tworek, Jacob Hilton, Reiichiro Nakano, Christopher Hesse, and John Schulman. 2021. Training verifiers to solve math word problems. *CoRR*, abs/2110.14168.

Damai Dai, Chengqi Deng, Chenggang Zhao, R. X. Xu, Huazuo Gao, Deli Chen, Jiashi Li, Wangding Zeng, Xingkai Yu, Y. Wu, Zhenda Xie, Y. K. Li, Panpan Huang, Fuli Luo, Chong Ruan, Zhifang Sui, and Wenfeng Liang. 2024. Deepseekmoe: Towards ultimate expert specialization in mixture-of-experts language models. In *Proceedings of the 62nd Annual Meeting of the Association for Computational Linguistics (Volume 1: Long Papers), ACL 2024, Bangkok, Thailand, August 11-16, 2024*, pages 1280–1297.

DeepSeek-AI, Aixin Liu, Bei Feng, Bin Wang, Bingxuan Wang, Bo Liu, Chenggang Zhao, Chengqi Deng, Chong Ruan, Damai Dai, Daya Guo, Dejian Yang, Deli Chen, Dongjie Ji, Erhang Li, Fangyun Lin, Fuli Luo, Guangbo Hao, Guanting Chen, Guowei Li, Hao Zhang, Hanwei Xu, Hao Yang, Haowei Zhang, Honghui Ding, Huajian Xin, Huazuo Gao, Hui Li, Hui Qu, J. L. Cai, Jian Liang, Jianzhong Guo, Jiaqi Ni, Jiashi Li, Jin Chen, Jingyang Yuan, Junjie Qiu, Junxiao Song, Kai Dong, Kaige Gao, Kang Guan, Lean Wang, Lecong Zhang, Lei Xu, Leyi Xia, Liang Zhao, Liyue Zhang, Meng Li, Miaojun Wang, Mingchuan Zhang, Minghua Zhang, Minghui Tang, Mingming Li, Ning Tian, Panpan Huang, Peiyi Wang, Peng Zhang, Qihao Zhu, Qinyu Chen, Qiushi Du, R. J. Chen, R. L. Jin, Ruiqi Ge, Ruizhe Pan, Runxin Xu, Ruyi Chen, S. S. Li, Shanghao Lu, Shangyan Zhou, Shanhuang Chen, Shaoqing Wu, Shengfeng Ye, Shirong Ma, Shiyu Wang, Shuang Zhou, Shuiping Yu, Shunfeng Zhou, Size Zheng, Tao Wang, Tian Pei, Tian Yuan, Tianyu Sun, W. L. Xiao, Wangding Zeng, Wei An, Wen Liu, Wenfeng Liang, Wenjun Gao, Wentao Zhang, X. Q. Li, Xiangyue Jin, Xianzu Wang, Xiao Bi, Xiaodong Liu, Xiaohan Wang, Xiaojin Shen, Xiaokang Chen, Xiaosha Chen, Xiaotao Nie, and Xiaowen Sun. 2024. Deepseek-v2: A strong, economical, and efficient mixture-of-experts language model. *CoRR*, abs/2405.04434.

William Fedus, Barret Zoph, and Noam Shazeer. 2022. Switch transformers: Scaling to trillion parameter models with simple and efficient sparsity. *J. Mach. Learn. Res.*, 23:120:1–120:39.

Gayathrimanoj. 2023. dataset_shell. https://huggingface.co/datasets/gayathrimanoj/dataset_shell.

Gkamradt. 2023. Needle in a haystack - pressure testing llms. https://github.com/gkamradt/LLMTest_NeedleInAHaystack/tree/main.

Dan Hendrycks, Collin Burns, Steven Basart, Andy Zou, Mantas Mazeika, Dawn Song, and Jacob Steinhardt. 2021a. Measuring massive multitask language understanding. In *ICLR*.

Dan Hendrycks, Collin Burns, Saurav Kadavath, Akul Arora, Steven Basart, Eric Tang, Dawn Song, and Jacob Steinhardt. 2021b. Measuring mathematical problem solving with the MATH dataset. In *NeurIPS*.

Jiaming Ji, Mickel Liu, Josef Dai, Xuehai Pan, Chi Zhang, Ce Bian, Boyuan Chen, Ruiyang Sun, Yizhou Wang, and Yaodong Yang. 2023. Beavertails: Towards improved safety alignment of LLM via a human-preference dataset. In *NeurIPS*.

Albert Q. Jiang, Alexandre Sablayrolles, Antoine Roux, Arthur Mensch, Blanche Savary, Chris Bamford, Devendra Singh Chaplot, Diego de Las Casas, Emma Bou Hanna, Florian Bressand, Gianna Lengyel, Guillaume Bour, Guillaume Lample, Lélio Renard Lavaud, Lucile Saulnier, Marie-Anne Lachaux, Pierre Stock, Sandeep Subramanian, Sophia Yang, Szymon Antoniak, Teven Le Scao, Théophile Gervet, Thibaut Lavril, Thomas Wang, Timothée Lacroix, and William El Sayed. 2024. Mixtral of experts. *CoRR*, abs/2401.04088.

Dmitry Lepikhin, HyoukJoong Lee, Yuanzhong Xu, Dehao Chen, Orhan Firat, Yanping Huang, Maxim Krikun, Noam Shazeer, and Zhifeng Chen. 2021. Gshard: Scaling giant models with conditional computation and automatic sharding. In *ICLR*.

Anton Lozhkov, Raymond Li, Loubna Ben Allal, Federico Cassano, Joel Lamy-Poirier, Nouamane Tazi, Ao Tang, Dmytro Pykhtar, Jiawei Liu, Yuxiang Wei, Tianyang Liu, Max Tian, Denis Kocetkov, Arthur

Zucker, Younes Belkada, Zijian Wang, Qian Liu, Dmitry Abulkhanov, Indraneil Paul, Zhuang Li, Wen-Ding Li, Megan Risdal, Jia Li, Jian Zhu, Terry Yue Zhuo, Evgenii Zheltonozhskii, Nii Osae Osae Dade, Wenhao Yu, Lucas Krauß, Naman Jain, Yixuan Su, Xuanli He, Manan Dey, Edoardo Abati, Yekun Chai, Niklas Muennighoff, Xiangru Tang, Muhtasham Oblokulov, Christopher Akiki, Marc Marone, Chenghao Mou, Mayank Mishra, Alex Gu, Binyuan Hui, Tri Dao, Armel Zebaze, Olivier Dehaene, Nicolas Patry, Canwen Xu, Julian J. McAuley, Han Hu, Torsten Scholak, Sébastien Paquet, Jennifer Robinson, Carolyn Jane Anderson, Nicolas Chapados, and et al. 2024. Starcoder 2 and the stack v2: The next generation. *CoRR*, abs/2402.19173.

Xuezhe Ma, Chunting Zhou, Xiang Kong, Junxian He, Liangke Gui, Graham Neubig, Jonathan May, and Luke Zettlemoyer. 2022. Mega: moving average equipped gated attention. *arXiv preprint arXiv:2209.10655*.

Meta AI. 2024. Introducing meta llama 3: The most capable openly available llm to date. https://ai.meta.com/blog/meta-llama-3/. Accessed: 2024-04-20.

Mosaic Research Team. 2024. Introducing DBRX: A new state-of-the-art open LLM. https://www.databricks.com/blog/introducing-dbrx-new-state-art-open-llm. Accessed: 2024-03-27.

Keiran Paster, Marco Dos Santos, Zhangir Azerbayev, and Jimmy Ba. 2024. Openwebmath: An open dataset of high-quality mathematical web text. In *ICLR*.

Colin Raffel, Noam Shazeer, Adam Roberts, Katherine Lee, Sharan Narang, Michael Matena, Yanqi Zhou, Wei Li, and Peter J Liu. 2020. Exploring the limits of transfer learning with a unified text-to-text transformer. *Journal of machine learning research*, 21(140):1–67.

Baptiste Rozière, Jonas Gehring, Fabian Gloeckle, Sten Sootla, Itai Gat, Xiaoqing Ellen Tan, Yossi Adi, Jingyu Liu, Tal Remez, Jérémy Rapin, Artyom Kozhevnikov, Ivan Evtimov, Joanna Bitton, Manish Bhatt, Cristian Canton-Ferrer, Aaron Grattafiori, Wenhan Xiong, Alexandre Défossez, Jade Copet, Faisal Azhar, Hugo Touvron, Louis Martin, Nicolas Usunier, Thomas Scialom, and Gabriel Synnaeve. 2023. Code llama: Open foundation models for code. *CoRR*, abs/2308.12950.

Noam Shazeer, Azalia Mirhoseini, Krzysztof Maziarz, Andy Davis, Quoc V. Le, Geoffrey E. Hinton, and Jeff Dean. 2017. Outrageously large neural networks: The sparsely-gated mixture-of-experts layer. In *ICLR*.

Hugo Touvron, Thibaut Lavril, Gautier Izacard, Xavier Martinet, Marie-Anne Lachaux, Timothée Lacroix, Baptiste Rozière, Naman Goyal, Eric Hambro, Faisal Azhar, et al. 2023. Llama: Open and efficient foundation language models. *arXiv preprint arXiv:2302.13971*.

Ashish Vaswani, Noam Shazeer, Niki Parmar, Jakob Uszkoreit, Llion Jones, Aidan N Gomez, Łukasz Kaiser, and Illia Polosukhin. 2017. Attention is all you need. *Advances in neural information processing systems*, 30.

Yizhong Wang, Yeganeh Kordi, Swaroop Mishra, Alisa Liu, Noah A. Smith, Daniel Khashabi, and Hannaneh Hajishirzi. 2023a. Self-instruct: Aligning language models with self-generated instructions. In *ACL*, pages 13484–13508.

Zengzhi Wang, Rui Xia, and Pengfei Liu. 2023b. Generative AI for math: Part I - mathpile: A billion-token-scale pretraining corpus for math. *CoRR*, abs/2312.17120.

Yuxiang Wei, Zhe Wang, Jiawei Liu, Yifeng Ding, and Lingming Zhang. 2024. Magicoder: Empowering code generation with oss-instruct. In *ICML*.

Can Xu, Qingfeng Sun, Kai Zheng, Xiubo Geng, Pu Zhao, Jiazhan Feng, Chongyang Tao, Qingwei Lin, and Daxin Jiang. 2024. Wizardlm: Empowering large pre-trained language models to follow complex instructions. In *The Twelfth International Conference on Learning Representations, ICLR 2024, Vienna, Austria, May 7-11, 2024*.

Yifan Zhang. 2024. StackMathQA: A Curated Collection of 2 Million Mathematical Questions and Answers Sourced from Stack Exchange. https://github.com/yifanzhang-pro/StackMathQA. Accessed: 2024-03-26.

Tianyu Zheng, Ge Zhang, Tianhao Shen, Xueling Liu, Bill Yuchen Lin, Jie Fu, Wenhu Chen, and Xiang Yue. 2024. Opencodeinterpreter: Integrating code generation with execution and refinement. In *ACL*, pages 12834–12859.

Yanqi Zhou, Tao Lei, Hanxiao Liu, Nan Du, Yanping Huang, Vincent Y. Zhao, Andrew M. Dai, Zhifeng Chen, Quoc V. Le, and James Laudon. 2022. Mixture-of-experts with expert choice routing. In *Advances in Neural Information Processing Systems 35*.

A Symbol in equations

Symbol	Explaination
A	Accumulate Time
T_s	Tensor Parallel Size
S	Sequence Length
D_s	Data Parallel Size
V	Vocab Size
BW_{link}	Bi-directional internal link BW
L	Layer Number
BW_{net}	Net bandwidth
P_s	Pipeline Parallel Size
n_{net}	Num net connector
B	Micro Batch Size
H	Hidden Size
T_0/s	Forward and backward compute time
T_1/s	Pipeline bubble
T_2/s	Pipeline parallel communication time
T_3/s	Tensor parallel communication time
T_4/s	Data parallel communication time
F/TFlops	Floating-point performance of a model with the same architecture but smaller size on a GPU

Table 9: Symbol in equations.

B Details for Training

Parameter	Pre-train	Fine-tune
Learning rate (LR)	1.0e-5∼1.0e-4	8.0e-5
LR decay style	cosine	constant
Sequence length	4096	16384
Global Batch size	1536	1152

Table 10: Training hyper-parameters.

C Details for Pre-training data

Web (25.2%). Website crawling data is a collection from open source datasets and the common crawl data processed in our previous works (Yuan 1.0). Please refer to Yuan 1.0 for more details about the Massive Data Filtering System (MDFS) that extract contents in higher quality from web contexts.

Encyclopedia (1.2%), **thesis** (0.84%), **book** (6.4%) and **translation** (1.1%) data are inherited from Yuan 1.0 and Yuan 2.0 datasets.

Code (47.5%). The code dataset is greatly expanded compared with Yuan 2.0. We adopt code from the Stack v2 (Lozhkov et al., 2024). The comments in Stack v2 are translated into Chinese. Code synthesized data created with the similar method as in Yuan 2.0.

Math (6.36%). All math data from Yuan 2.0 is reused. The data are predominantly from open source datasets, including proof-pile v1 (Azerbayev et al., 2022) and v2 (Paster et al., 2024), AMPS (Hendrycks et al., 2021b), Math-Pile (Wang et al., 2023b) and StackMathQA (Zhang, 2024). A synthetic dataset for numerical calculation is created with Python to benefit for four arithmetic operations.

Specific-domain (1.93%) is a dataset with knowledge from different background.

D Details for Fine-tuning data

Code Instruction dataset. All the coding data with Chinese instruction and parts with English comments is generated with LLMs. About 30% of the code instruction data is in English, and the rest is in Chinese. The synthetic data are fabricated in a way that imitates the Python code with Chinese comments in terms of prompt generation and data cleaning strategy.

- Python code with English comments is collected from Magicoder-Evol-Instruct-110K (Wei et al., 2024) and CodeFeedback-Filtered-Instruction (Zheng et al., 2024). The instruction data with language tag such as "python" is extracted from the dataset, and organized into the format as shown in Appendix E. The dataset is also expanded with the Evol-instruct (Xu et al., 2024) and Self-instruct (Wang et al., 2023a) method applied in the construction of Chinese Python code.

- Other codes such as C/C++/Go/Java/SQL/Shell etc., with English comments from open source dataset (Wei et al., 2024; Zheng et al., 2024; b-mc2, 2023; Clinton, 2023; Gayathrimanoj, 2023; Byroneverson, 2024) are processed in a similar way with Python code. The cleaning strategies are similar to the method in Yuan 2.0. A sandbox is designed to extract compilable and executable lines in the generated codes, and keep the lines that pass at least one unit test.

Math Instruction dataset. The math instruction dataset are all inherited from the fine-tuning dataset in Yuan 2.0. To improve the ability of model to solve mathematical problems with programmatic methods, we construct a Program of Thoughts (PoT) prompting math data (Chen et al., 2023). PoT converts the mathematic problem into a code generation task that do calculations with Python.

Safety Instruction dataset. In addition to the chat dataset of Yuan 2.0, we construct a bilingual safe alignment dataset based on an open source safe alignment dataset (Ji et al., 2023). We only take the questions from the public dataset, and increase the variety of questions and regenerate Chinese and English answers with large language models.

E Prompt Examples for Downstream Tasks

Code generation

> Instruction: Given two positive integers a and b, return the even digits between a and b, in ascending order.
> For example:
> generate_integers(2, 8) => [2, 4, 6, 8]
> generate_integers(8, 2) => [2, 4, 6, 8]
> generate_integers(10, 14) => []
> Response:
> <sep>
> ```python
> def generate_integers(a, b):

MMLU

> Glucose is transported into the muscle cell:<n> A. via protein transporters called GLUT4. <n> B. only in the presence of insulin. <n> C. via hexokinase. <n>D. via monocarbylic acid transporters. <sep> A.

ARC-C

> few-shot examples<n> question<n> optionA<n> optionB<n> optionC<n> optionD<sep> answer